Elastic scattering of polarized neutrons on ^{16}O, ^{59}Co, and Pb at 23 MeV

S. T. Lam, W. K. Dawson, S. A. Elbakr,* H. W. Fielding, P. W. Green, R. L. Helmer,† I. J. van Heerden,‡ A. H. Hussein,§ S. P. Kwan,** G. C. Neilson, T. Otsubo,†† D. M. Sheppard, H. S. Sherif, and J. Soukup
Nuclear Research Centre, University of Alberta, Edmonton, Alberta, Canada T6G 2N5
(Received 21 January 1985)

Differential cross sections and analyzing powers of neutrons elastically scattered from ^{16}O, ^{59}Co, and Pb were measured using two 183 cm long position sensitive scintillators. A beam of polarized neutrons ($P=0.51$, $E_n=23$ MeV) was produced by the $^3H(d,n)^4He$ reaction. A superconducting solenoid was used to precess the neutron spin by 180° for the determination of analyzing powers. After correcting for neutron flux attenuation and multiple scattering due to the finite size of the scatterers, the data were analyzed using a conventional optical model potential.

I. INTRODUCTION

It has long been recognized that polarization studies are crucial for an accurate determination of the characteristics of the spin-orbit part of the nucleon-nucleus interaction. A few years ago Roman[1] raised the question concerning the shape of the spin-orbit part of the neutron optical potential. To shed light on this point one must have accurate neutron-nucleus analyzing power data. The recent work of Floyd *et al.*[2] for neutron scattering on light nuclei (^9Be, ^{12}C, and ^{40}Ca) indicates that if the spin-orbit interaction is restricted to the conventional Thomas form, the diffuseness a_{so} is unusually small as compared with global values; this small value of a_{so} is in agreement with the conjecture made by Roman. Good quality neutron data could also determine other details of the potential such as the presence of an imaginary term in the spin-orbit potential at low neutron energies. This has been discussed by Floyd *et al.*,[2,3] Delaroche *et al.*,[4] and Mackintosh and Kobos.[5]

Analyzing powers and differential cross sections were measured for 23 MeV neutrons elastically scattered from ^{16}O, ^{59}Co, and Pb in the present investigation. Optical potential analysis of the data was carried out using the computer code MAGALI (Ref. 6) with an aim to elucidate the spin-orbit part of the potential.

II. EXPERIMENTAL PROCEDURE

A pulsed beam of polarized neutrons was obtained from the $^3H(d,n)^4He$ reaction. The pulsed deuteron beam was derived from a CN Van de Graaff accelerator with a Mobley magnet compression system. The target was a tritium gas cell cooled to liquid nitrogen temperature. At an incident deuteron energy of 7 MeV and an angle of 30° to the incident beam, the resulting neutron energy is 23 MeV and the beam polarization is 0.51 ± 0.02. A description of the neutron facility has been reported by Soukup *et al.*[7]

A schematic drawing of the experimental setup is shown in Fig. 1. A superconducting solenoid placed at 30° to the incident deuteron beam was used to precess the neutron spin through 180°. All scattering samples were cylindrical in shape, 3.81 cm in length and in diameter, and were placed just beyond the superconducting solenoid with the axis of the cylinder along the direction of the incident neutron beam. The distance between the tritium gas cell and the scatterer was 122 cm. The scattered neutrons were detected by two 183 cm long, 7.62 cm diameter, NE213 liquid scintillators. One scintillator at a distance of 401 cm from the scatterer covered a scattering angular range of 13.6° to 37.8°, and the other at a distance of 327 cm covered 56.5° to 84.0°. Massive steel shielding was placed around the tritium gas cell and the scintillators. The aperture at 30° was lined with heavy metal so that the solid angle of the neutron beam at the scatterer position was slightly larger than the solid angle subtended by the scatterer.

Neutron time-of-flight technique and n-γ pulse-shape discrimination were used in the detection of neutrons. An RCA 8854 photomultiplier tube was used to view the scintillation signal at each end of the long scintillators. The time difference of the scintillation signal as observed by the two photomultiplier tubes gives the position of the

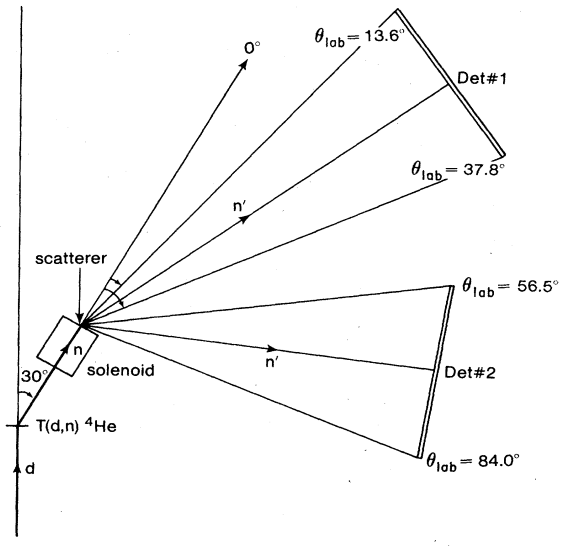

FIG. 1. A schematic drawing of the experiment.

scintillation. Since a pulsed beam of deuterons was used to produce the neutrons, neutron time-of-flight circuits were set up between the pulsed beam pickoff and each of the left and right photomultipliers. Signals from the left and right time-of-flight circuits, the n-γ pulse-shape discrimination, and the amplitude of the scintillation were recorded event by event on magnetic tape.

Differential cross sections and analyzing powers were determined for neutrons elastically scattered from natural samples of H_2O, D_2O, Co, and Pb. Measurements with scatterer in and scatterer out were carried out for background subtraction, and measurements with solenoid magnetic field on and field off were carried out to determine analyzing powers. A neutron monitor placed at a fixed position was used for normalization.

Since the long scintillators were placed at different distances from the scatterer and subtended a chord instead of an arc, the difference in geometrical effect was corrected by measuring the γ-ray intensity emitted by a PuBe source placed at the scatterer position.

III. RESULTS

The long scintillator placed at the forward angle was divided for analysis into 16 segments giving measurements of 16 angles, each segment subtending 1.5° at the scatterer. This division is justified by the 18 ns which it takes for a scintillation signal to travel from one end of the long scintillator to the other and the system timing resolution of approximately 1 ns if a small detector is used. Since the neutron count rate decreases rapidly at larger angles, the other long scintillator was divided for analysis into eight segments, with each segment subtending an angle of 3.4°. The energy bias for all segments of both scintillators was set at approximately 9 MeV energy.

H_2O and D_2O were used as scatterers for the measurement of differential cross sections and analyzing powers of n-O elastic scattering. The n-H and n-D results in the present measurement were compared with the n-H differential cross sections determined by Flynn and Bendt[8] and Scanlon *et al.*[9] and with the n-D differential cross sections determined by Seagrave *et al.*[10] and Burrows.[11] After a normalization factor was determined, absolute differential cross sections were evaluated for n-O, n-Co, and n-Pb elastic scatterings.

In the ^{3}H(d,n)^{4}He reaction at $\theta_n = 30°$, the neutron polarization varies smoothly from 0.50 to 0.53 with an uncertainty of ± 0.02 for deuteron energies from 6.5 to 7.0 MeV.[12,13] Because of the energy loss in the thin foil of the gas cell and in the tritium gas by the 7.0 MeV incident deuteron beam, the deuteron energy at the middle of the gas cell was about 6.7 MeV. By interpolating the polarization values between deuteron energies of 6.5 and 7.0 MeV, the neutron beam polarization was estimated to be 0.51. This value was used in the determination of analyzing powers for n-O, n-Co, and n-Pb elastic scattering.

Since a fairly large scatterer was used in the experiment, effects due to flux attenuation of the incident neutron beam and multiple scattering of neutrons in the scatterer had to be evaluated in order to make corrections to the measured differential cross sections and analyzing powers. The computer code PMS1 (Ref. 14) was used for such corrections. The original program written by Miller *et al.*[15] was modified to accommodate the present experimental geometry. It uses a Monte Carlo technique and

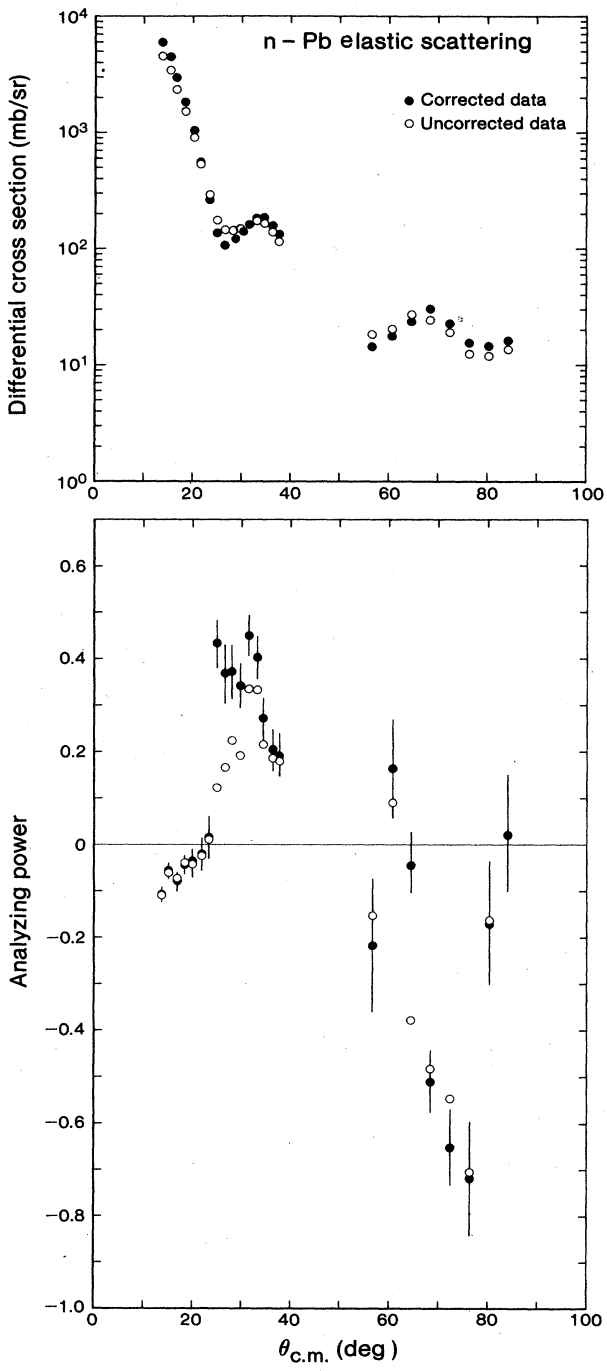

FIG. 2. A comparison between the corrected and uncorrected differential cross sections and analyzing powers for n-Pb elastic scattering. The correction is for flux attenuation of the incident neutron beam and neutron multiple scattering in the scatterer. The errors in the differential cross sections are smaller than the size of the circle. For reason of clarity, only the errors for the corrected analyzing powers are shown.

flux estimation to simulate the experimental situation. The differential cross section for n-Pb elastic scattering is increased by about 30%, n-Co by about 10%, and n-O by about 8% at the forward angles, while at angles around the first minimum, the differential cross sections are reduced by about the same percentages. The correction to the analyzing powers increases the amplitudes of the maximum and minimum values and is mostly smaller than the statistical uncertainty of the measured analyzing powers. A comparison between the corrected and uncorrected differential cross sections and analyzing powers for the case of n-Pb elastic scattering is shown in Fig. 2.

The differential cross sections and angular distributions of analyzing powers for n-O, n-Co, and n-Pb elastic scatterings at a neutron energy of 23 MeV determined in the present measurement are shown in Figs. 3—5. The errors in the differential cross section are about 3—4% except near the minimum, where they may be as large as

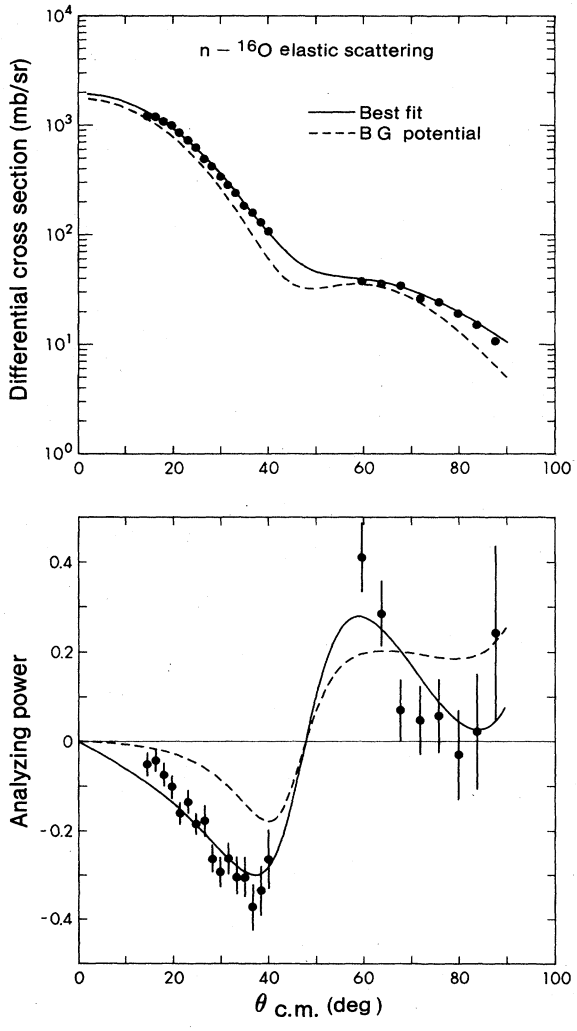

FIG. 3. Differential cross sections and angular distribution of analyzing powers for n-^{16}O elastic scattering at $E_n = 23$ MeV. The dashed curve gives the result of the calculation using optical potential parameters from Becchetti and Greenlees and the solid curve the result from best fit parameters.

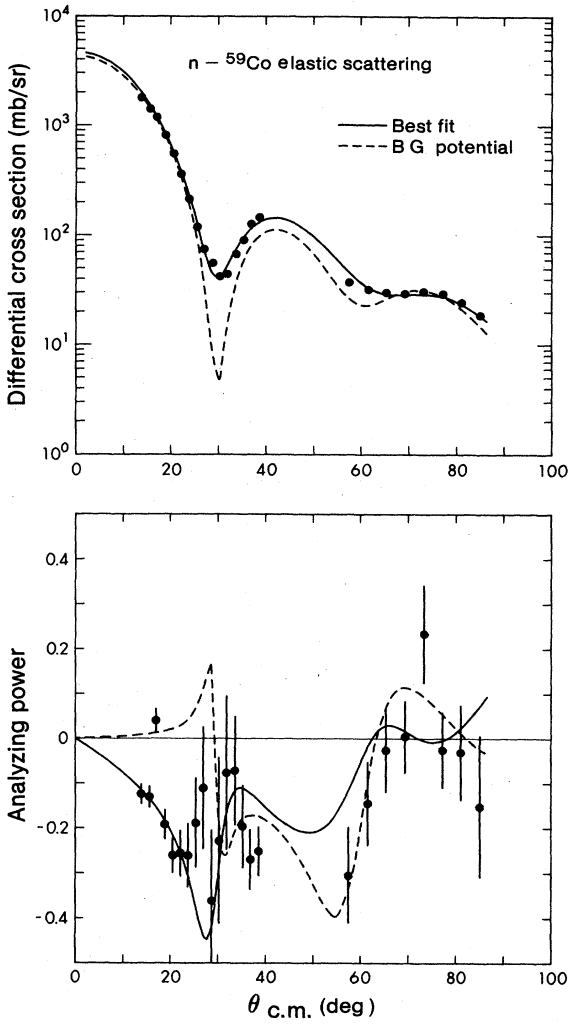

FIG. 4. Differential cross sections and angular distribution of analyzing powers for n-^{59}Co elastic scattering at $E_n = 23$ MeV. The dashed curve gives the result of the calculation using optical potential parameters from Becchetti and Greenlees and the solid curve the result from best fit parameters.

8—10%. The errors in the analyzing power are mainly due to statistics. They are about ±0.03 at smaller angles and about ±0.1 at larger angles. Since the scatterers were made from natural materials, the Pb scatterer (52% ^{208}Pb, 22% ^{207}Pb, 25% ^{206}Pb) combined the effect of several isotopes. The Co scatterer is isotopically pure, i.e., ^{59}Co only, and the O scatterer is 99.76% ^{16}O.

Since the time resolution for each bin of the first long scintillator was about 1.1 ns and that for the second long scintillator was about 2.2 ns, the inelastic and elastic neutron peaks in the time-of-flight spectrum were resolved for n-^{16}O and n-^{208}Pb scatterings, but not in the case of n-^{59}Co, n-^{206}Pb, and n-^{207}Pb. El-Kadi *et al.*[16] measured the inelastic neutron scattering cross sections for isotopes of Fe and Cu at neutron energies of 8 to 14 MeV and found the cross sections to be about 10 mb/sr or less throughout their angular range and not varying much with neutron energy. Hence it is assumed that the inelas-

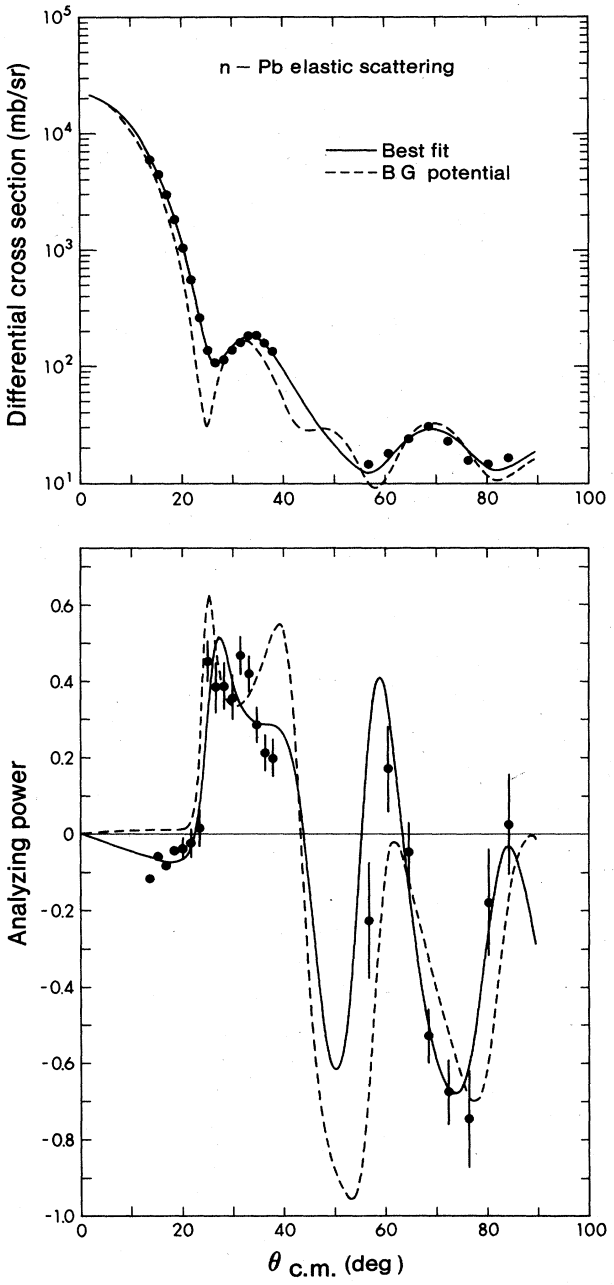

FIG. 5. Differential cross sections and angular distribution of analyzing powers for n-Pb elastic scattering at $E_n=23$ MeV. The dashed curve gives the result of the calculation using optical potential parameters from Becchetti and Greenlees and the solid curve the result from best fit parameters.

tic neutron contribution to the elastic peak is small in the present measurement of n-^{59}Co and n-Pb elastic scatterings except near the minima of the differential cross sections. The effect of the inelastic neutrons on the results of the optical model analysis will be examined in the next section.

The unusually large positive analyzing power around 20° observed by Begum *et al.*[17] at a neutron energy of 16.1 MeV is not seen in the present measurement. The variation of the analyzing power in this angular region is quite smooth in ^{16}O and Pb. The analyzing power at 17° in ^{59}Co is slightly positive and inconsistent with the other data points in this angular region. It is possible that there is a spurious error with this data point.

IV. OPTICAL MODEL ANALYSIS

The computer code MAGALI (Ref. 6) was used in the optical model analysis of the data. The form of the optical potential used is

$$U=-Vf(r,r_v,a_v)-i\left[W_v-4a_wW_D\frac{d}{dr}\right]f(r,r_w,a_w)$$
$$+2\lambda_\pi^2V_{so}\frac{1}{r}\frac{d}{dr}f(r,r_{so},a_{so})\mathbf{l}\cdot\mathbf{s}\ , \qquad (1)$$

where V, W_v, W_D, and V_{so} are, respectively, the depths of the real, imaginary volume, imaginary surface, and spin-orbit parts of the potential, and $f(r,r_i,a_i)$ are of the Woods-Saxon shape given by

$$f(r,r_i,a_i)=\{1+\exp[(r-r_iA^{1/3})/a_i]\}^{-1}\ .$$

The finite angular spread in the angle subtended by the different segments of the long scintillators was taken into account in the calculation.

Of all the global sets of optical model potentials for neutron-nucleus scattering, the set by Becchetti and Greenlees[18] has most often been used in making comparison with other optical model potentials. Although new global sets have been developed by Ohio[19] and TUNL,[16] they are, however, similar in nature and their geometry parameters do not differ significantly from each other. For this reason the set by Becchetti and Greenlees is chosen as representative of the global behavior of optical model calculations.

The differential cross sections and angular distributions of analyzing powers calculated using the global parameters of Becchetti and Greenlees for neutron elastic scatterings of ^{16}O, ^{59}Co, and Pb at 23 MeV are shown as dashed curves in Figs. 3–5. Since the variation of the global parameters is small for the different isotopes of Pb, the parameters corresponding to ^{208}Pb were used in the Pb calculation. The calculation underestimates the cross sections and gives deeper minima for all three scatterers. The calculated values of the analyzing powers generally follow the trend of the experimental variation in ^{16}O and Pb, but in ^{59}Co the calculated analyzing powers have the opposite sign to that of the measurement for angles between 14° and 30°. Other global parameter sets[16,19] were also used in the calculation and produced similar results.

The computer code MAGALI was used to obtain optimum optical model parameters by fitting the data using the global sets as initial parameters. The optimum set was arrived at only after using the search routine repeatedly with parameters from the previous search as a guide. Hence the final values of the optimum parameters had no bearing to which global set was used initially. Since the cross section data were more accurately determined than the analyzing power data, weighting using the respective errors could only give good fits to the differential cross

sections but not the analyzing powers. This is due to the fact that the χ^2 from the cross section data is much larger than the χ^2 from the analyzing power data, resulting in a domination of the cross section data in the fitting process. By increasing the weighting factor of the analyzing power data to 5, reasonable fits to the analyzing power data could now be achieved while good fits to the cross section data could still be maintained. Even though the analyzing power data were not determined as accurately as the cross section data, the inclusion of analyzing power data in the optical model analysis is important so as to give credence to the determined values of the spin-orbit potential. The best fit results for ^{16}O, ^{59}Co, and Pb are shown as solid curves in Figs. 3—5.

An extensive search was carried out to fit our present data with an average geometry for all three nuclei without success, indicating that the structure of individual nuclei may cause the geometry to change from nucleus to nucleus. As shown in Figs. 3—5, the results of the calculation using the global set by Becchetti and Greenlees can only give the general shapes of the experimental distributions. This is also true for the other two global sets. The failure of using global parameter sets to precisely describe neutron data has been reported (see, for example, Ref. 21).

Table I gives a tabulation of the global set by Becchetti and Greenlees, global set A of Ohio,[19] and the optimum parameters determined presently for ^{16}O, ^{59}Co, and Pb. The global sets from TUNL (Ref. 16) are not listed for comparison, since in the TUNL optical potential the geometry parameters for the imaginary volume part of the potential are chosen the same as the geometry parameters of the real part of the potential. This is different from the form of the volume imaginary potential given in Eq. (1), where the same geometry parameters are used for both the imaginary volume and imaginary surface parts of the potential. The global sets of Becchetti and Greenlees and of Ohio use the same form as in Eq. (1).

The χ^2 per data point is also tabulated in Table I. It is used as a criterion to judge the quality of fit between calculations and experimental data. The optical model calculations using global set A of Ohio give a slightly better fit to the data than those of Becchetti and Greenlees. In global set B of Ohio, an A dependence is allowed for the radius parameter of the real part of the potential instead of a fixed value for all A. Calculations using global set B do not fit the data as well as set A. The fit for set B is approximately the same as the fit for Becchetti and Greenlees. The quality of fit to the data using the global sets of TUNL is about the same as global set A of Ohio.

Since the optical potential parameters derived from a search routine are not unique, the uncertainties of the parameters were determined as follows. The geometry parameters were changed one at a time from their optimum values while the rest of the parameters were set free in the search program in order to arrive at another minimum χ^2. The uncertainty in that parameter was then determined from its extreme values that still gave a reasonably good fit to the data.

Most of the present geometry parameters agree with the average geometry parameters of the global sets within the uncertainty determined as described in the preceding paragraph. The significant difference is that the present radius and diffuseness parameters for the imaginary potential are larger in ^{16}O and smaller in Pb than the global pa-

TABLE I. Optical potential parameters from Becchetti and Greenlees, global set A of Ohio, and the best fit parameters from the present search using MAGALI. The well depths are in MeV and the radii and diffuseness parameters in fm. χ^2_σ/N and χ^2_A/N are, respectively, the chi squares per data point from differential cross sections and analyzing powers. J_v/A and J_w/A are, respectively, the real and imaginary volume integrals per nucleon and $J_{so}/A^{1/3}$ the spin-orbit volume integral divided by the one-third power of the mass number. Their units are in MeV fm^3.

	^{16}O			^{59}Co			Pb		
Parameter	BG	Ohio set A	Present	BG	Ohio set A	Present	BG	Ohio set A	Present
V	48.91	46.60	42.91	46.87	45.05	34.20	43.83	42.72	38.91
r_v	1.17	1.198	1.183	1.17	1.198	1.346	1.17	1.198	1.268
a_v	0.75	0.663	0.668	0.75	0.663	0.697	0.75	0.663	0.509
W_v	3.52	4.44	4.64	3.52	4.44	4.819	3.52	4.44	0.376
W_D	7.23	5.03	0.68	6.21	4.15	8.757	4.69	2.83	14.95
r_w	1.26	1.295	1.390	1.26	1.295	1.249	1.26	1.295	1.069
a_w	0.58	0.59	0.861	0.58	0.59	0.341	0.58	0.59	0.349
V_{so}		6.20	5.18		6.20	4.40		6.20	6.47
r_{so}		1.01	1.003		1.01	1.212		1.01	1.128
a_{so}		0.75	0.36		0.75	0.457		0.75	0.470
J_v/A	538	495	445^{+12}_{-15}	399	389	410^{+42}_{-40}	328	334	347^{+11}_{-20}
J_w/A	189	163	110^{+13}_{-15}	111	101	102^{+20}_{-7}	69	67	53^{+5}_{-7}
$J_{so}/A^{1/3}$		157	131^{+0}_{-15}		157	134^{+31}_{-50}		157	183^{+81}_{-33}
χ^2_σ/N	62	40	2.1	40	35	3.8	150	134	4.2
χ^2_A/N	12	12	1.4	11	11	1.5	11	10	2.2

rameters listed in Table I. The spin-orbit diffuseness parameter is also found to be small for all three nuclei in this investigation, supporting the finding of the TUNL group[2] and the conjecture of Roman.[1] In a recent analysis of n-^{208}Pb elastic scattering at 10 MeV, Delaroche *et al.*[4] arrived at values of 0.491 and 0.520 fm for a_{so}, which is in agreement with our value of 0.470 fm for Pb. a_{so} is particularly small for ^{16}O, which is in agreement with recent analysis on very light nuclei.[22,23]

Both volume and surface terms of the imaginary potential are found to be necessary. The variation of the surface well depth with respect to the volume well depth changes systematically from light to heavy nuclei. In ^{16}O the potential is mostly volume, in Pb it is mostly surface, while in ^{59}Co the two contributions are comparable. The well depths for W_v and W_D do not agree with the predictions of the global sets.[16,18,19]

The question of the necessity of an imaginary spin-orbit potential was also investigated. Since the data could be fitted equally well with and without an imaginary spin-orbit potential, we conclude that the requirement is not evident for 23 MeV neutrons using the standard shape of the optical potential. This is contrary to the findings of Floyd *et al.*[2,3] and Delaroche *et al.*,[4] who analyzed neutron scattering data of ^{54}Fe, ^{65}Cu, and ^{208}Pb at 10 and 14 MeV and concluded that a small positive W_{so} was required to fit the data. It is, however, possible that the requirement of an imaginary spin-orbit potential is energy dependent, as indicated in the analysis of proton data by Mackintosh and Kobos,[5] who used an l-dependent potential. In another work by the TUNL group, the result seems to show a reduction of the imaginary spin-orbit potential with an increase in neutron energy in the region of 10—14 MeV for ^{40}Ca elastic scattering.[21] This reduction is in the same trend as the variation for proton data and it is possible that the imaginary spin-orbit potential changes sign around 23 MeV in the case of neutrons. The existence of an imaginary spin-orbit potential is postulated in the microscopic calculation of Brieva and Rook,[24] and its strength is calculated to be 10—15 % of the real part of the spin-orbit potential, but the sign there is negative.

Because of the $V{\cdot}r^2$ and $W{\cdot}a_w$ type of ambiguities, it has been suggested[20] that the volume integral per nucleon of the potential is a better measure of the potential strength than the potential depth itself. The volume integrals per nucleon for different parts of the optical potential were calculated and are also tabulated in Table I. The errors in the volume integrals per nucleon were calculated from the uncertainties determined for the parameters.

The volume integrals per nucleon for ^{59}Co and Pb determined in the present analysis are about the same as those derived from the global sets.[16,18,19] However, for ^{16}O, the volume integrals per nucleon for all three parts (real, imaginary, and spin-orbit) of the optical potential are found to be smaller than the global values, supporting the conjecture that light nuclei may have different global properties.

From the analysis of the centroid energies of the bound single particle states and the results of the optical model analysis, Cooper and Hodgson[25] arrived at the following expression for the energy dependence of the spin-orbit potential:

$$V_{so}=(6.5\pm0.5)-(0.023\pm0.012)E \text{ MeV} ,$$

with $r_{so}=1.1$ fm and $a_{so}=0.62$ fm. In order to avoid the difference in the geometry parameters used, the volume integral, $J_{so}/A^{1/3}$, is calculated for the above relationship for 23 MeV neutrons and its value of 165 ± 16 MeV fm^3 compares well with the values for ^{59}Co and Pb in Table I, but not so well with the value for ^{16}O. This indicates once again that light nuclei may have different global behavior also in the spin-orbit potential strength.

Since the inelastic neutrons from the n-^{59}Co, n-^{206}Pb, and n-^{207}Pb were not separated from the elastic neutrons in the present measurement, a DWBA calculation[26] was used to estimate the inelastic cross sections in such nuclei. If the low-lying collective states of ^{59}Co are due to the coupling of an $f_{7/2}$ proton hole to the 2^+, first excited state of ^{60}Ni, we can use the description of the weak coupling between the proton hole and the vibrational core to calculate the inelastic cross section in ^{59}Co. Using the optical potential parameters determined presently for ^{59}Co and a deformation parameter of 0.211 (Ref. 27), the sum of the inelastic cross sections to the low-lying collective states was obtained. The sum of the inelastic cross sections varies smoothly from 14 to 1.5 mb/sr in our angular region and is about 10 mb/sr near 30°, where the first minimum of the differential cross section occurs. Hence the inelastic neutrons as estimated from calculation are contributing approximately 1—8 % to the measured elastic scattering cross section except near 30°, where the contribution is about 25%. The analyzing powers for the inelastic neutrons predicted from the DWBA calculations are small compared to the statistical errors in our angular region. In order to examine whether the inelastic neutron contribution affects the optical potential parameters determined by this experiment, the calculated inelastic cross sections were subtracted from the measured elastic cross sections and the resulting cross sections and the analyzing powers were fitted once again with the real, imaginary volume, and imaginary surface well depths set free while the rest of the parameters were kept the same as before. The well depths resulting from the search differed only slightly from the original values and were well within the uncertainties determined in the optical potential parameter sensitivity investigation.

Since the inelastic neutrons were separated from the elastic neutrons in n-^{208}Pb scattering, the inelastic cross sections were calculated only for n-^{206}Pb and n-^{207}Pb scatterings in the estimation of inelastic neutron contribution to n-Pb elastic scattering. Using the optical potential parameters determined presently for n-Pb elastic scattering and a deformation parameter of 0.037 (Ref. 27), the combined inelastic neutron scattering cross sections due to ^{206}Pb (25% natural abundance) and ^{207}Pb (22%) were found to vary smoothly from 1.5 to 0.1 mb/sr over our angular range. The calculated analyzing powers were again found to be small. Hence the unresolved inelastic neutrons as predicted by calculation are not significantly affecting the measured cross sections and analyzing powers of the n-Pb elastic scattering.

V. CONCLUSION

Differential cross sections and angular distributions of analyzing powers were measured for n-^{16}O, n-^{59}Co, and n-Pb elastic scatterings at 23 MeV. Optical model analysis using the global sets[16,18,19] cannot adequately reproduce the data distributions. Separate parameter sets are required to fit the data. Some deviations of the geometry parameters from the global values are observed, especially the small a_{so} obtained for the spin-orbit potential.

Recently Finlay *et al.*[28] investigated the energy dependence of the optical model parameters using n-^{208}Pb scattering in the energy range of 7—50 MeV and found energy variation in the geometry parameters. Calculations using their parameters interpolated for 23 MeV (Table II of Ref. 28) and their common geometry parameter set (Table III of Ref. 28) did not reproduce as detailed a fit to our data as is obtained in the present work. The quality of the fit, however, is slightly better than global set A of Ohio. On the other hand, the volume integrals per nucleon agree well with our values. This indicates that the global parameter sets are adequate for providing information on the gross behavior of the potential even though they may not reproduce the finer details of a specific data set.

This work was supported in part by the Natural Sciences and Engineering Research Council of Canada.

---

*On sabbatical leave from King Saud University, Riyad, Saudi Arabia.

†Now at TRIUMF, Simon Fraser University, Burnaby, British Columbia, Canada V5A 1S6.

‡Permanent address: University of the Western Cape, Bellville, 7530, South Africa.

§On sabbatical leave from University of Petroleum and Minerals, Dhahran, Saudi Arabia.

**Present address: Department of Physics, Queen's University, Kingston, Ontario, Canada K7L 3N6.

††Permanent address: National Defense Academy, Department of Physics, Hashirimizu, Yokosuka, Kanagawa, Japan.

[1]S. Roman, in *Lecture Notes in Physics,* edited by H. V. von Geramb (Springer, Berlin, 1979), Vol. 89, p. 258.

[2]C. E. Floyd, P. P. Guss, K. Murphy, R. C. Byrd, G. Tungate, S. A. Wender, R. L. Walter, and T. B. Clegg, Phys. Rev. Lett. **47**, 1042 (1981).

[3]C. E. Floyd, P. P. Guss, R. C. Byrd, K. Murphy, R. L. Walter, and J. P. Delaroche, Phys. Rev. C **28**, 1498 (1983).

[4]J. P. Delaroche, C. E. Floyd, P. P. Guss, R. C. Byrd, K. Murphy, G. Tungate, and R. L. Walter, Phys. Rev. C **28**, 1410 (1983).

[5]R. S. Mackintosh and A. M. Kobos, J. Phys. G **4**, L135 (1978).

[6]MAGALI—A Fortran IV Program for Automatic Search in Elastic Scattering Analysis with the Nuclear Optical Model for Spin 0-, 1/2-, and 1-particles, J. Raynal, Service de Physique Théorique, Centre d'Etudes Nucléaires de Saclay, Gif-sur-Yvette, France.

[7]J. Soukup, J. M. Cameron, S. T. Lam, and G. C. Neilson, Nucl. Instrum. Methods **141**, 409 (1977).

[8]E. R. Flynn and P. J. Bendt, Phys. Rev. **128**, 1268 (1962).

[9]J. P. Scanlon, G. H. Stafford, J. J. Thresher, P. H. Bowen, and A. Langsford, Nucl. Phys. **41**, 401 (1963).

[10]J. D. Seagrave, J. C. Hopkins, D. R. Dixon, P. W. Keaton, Jr., E. C. Kerr, A. Niiler, R. H. Sherman, and R. K. Walter, Ann. Phys. (N.Y.) **74**, 250 (1972).

[11]T. W. Burrows, Phys. Rev. C **8**, 1173 (1973).

[12]R. L. Walter, in *Proceedings of the Third International Symposium on Polarization Phenomena in Nuclear Reactions,* edited by H. H. Barschall and W. Haeberli (University of Wisconsin Press, Madison, 1970), p. 317.

[13]J. W. Sunier, R. V. Poore, R. A. Hardekopf, L. Morrison, G. C. Salzman, and G. G. Ohlsen, Phys. Rev. C **14**, 8 (1976).

[14]A. H. Hussein, private communication.

[15]T. G. Miller, F. P. Gibson, and G. W. Morrison, Nucl. Instrum. Methods **80**, 325 (1970).

[16]S. M. El-Kadi, C. E. Nelson, F. O. Purser, R. L. Walter, A. Beyerle, C. R. Gould, and L. W. Seagondollar, Nucl. Phys. **A390**, 509 (1982).

[17]A. Begum, R. B. Galloway, and F. K. McNeil-Watson, Nucl. Phys. **A332**, 349 (1979).

[18]F. D. Becchetti, Jr. and G. W. Greenlees, Phys. Rev. **182**, 1190 (1969).

[19]J. Rapaport, V. Kulkarni, and R. W. Finlay, Nucl. Phys. **A330**, 15 (1979).

[20]H. Feshbach, Annu. Rev. Nucl. Sci. **8**, 49 (1958).

[21]W. Tornow, E. Woye, G. Mack, C. E. Floyd, K. Murphy, P. P. Guss, S. A. Wender, R. C. Byrd, R. L. Walter, T. B. Clegg, and H. Leeb, Nucl. Phys. **A385**, 373 (1982).

[22]S. W. L. Leung and H. S. Sherif, Can. J. Phys. **56**, 1116 (1978).

[23]D. F. Jackson and I. Abdul-Jalil, J. Phys. G **6**, 481 (1980).

[24]F. A. Brieva and J. R. Rook, Nucl. Phys. **A307**, 493 (1978).

[25]S. G. Cooper and P. E. Hodgson, J. Phys. G **6**, L21 (1980).

[26]H. S. Sherif, Nucl. Phys. **A131**, 532 (1969).

[27]P. H. Stelson and L. Grodzins, Nucl. Data **1**, No. 1, 21 (1965).

[28]R. W. Finlay, J. R. M. Annand, T. S. Cheema, J. Rapaport, and F. S. Dietrich, Phys. Rev. C **30**, 796 (1984).